

## Band offsets and optical bowings of chalcopyrites and Zn-based II-VI alloys

Su-Huai Wei and Alex Zunger

Citation: *Journal of Applied Physics* **78**, 3846 (1995); doi: 10.1063/1.359901

View online: <http://dx.doi.org/10.1063/1.359901>

View Table of Contents: <http://scitation.aip.org/content/aip/journal/jap/78/6?ver=pdfcov>

Published by the AIP Publishing

---

### Articles you may be interested in

[Gain characteristics of gain-guided II-VI laser diodes](#)

*Appl. Phys. Lett.* **69**, 3893 (1996); 10.1063/1.117561

[Smooth etching of various III/V and II/VI semiconductors by Cl<sub>2</sub> reactive ion beam etching](#)

*J. Vac. Sci. Technol. B* **14**, 1764 (1996); 10.1116/1.588554

[Crystal-structure studies of II-VI semiconductors using angle-dispersive diffraction techniques with an image-plate detector](#)

*AIP Conf. Proc.* **309**, 633 (1994); 10.1063/1.46413

[Epitaxial growth of II-VI semiconductor superlattices by pulsed-laser deposition](#)

*AIP Conf. Proc.* **288**, 577 (1993); 10.1063/1.44857

[Electronic structure and stability of II-VI semiconductors and their alloys: The role of metal d bands](#)

*J. Vac. Sci. Technol. A* **6**, 2597 (1988); 10.1116/1.575515

---



Frustrated by old technology? Is your AFM dead and can't be repaired? Sick of bad customer support?

**It is time to upgrade your AFM**  
Minimum \$20,000 trade-in discount for purchases before August 31st

**Asylum Research is today's technology leader in AFM**

**OXFORD INSTRUMENTS**  
The Business of Science®

[dropmyoldAFM@oxinst.com](mailto:dropmyoldAFM@oxinst.com)

# Band offsets and optical bowings of chalcopyrites and Zn-based II-VI alloys

Su-Huai Wei<sup>a)</sup> and Alex Zunger

National Renewable Energy Laboratory, Golden, Colorado 80401

(Received 20 December 1994; accepted for publication 2 June 1995)

Using first-principles band-structure theory we have systematically calculated the (i) alloy bowing coefficients, (ii) alloy mixing enthalpies, and (iii) interfacial valence- and conduction-band offsets for three mixed-anion ( $\text{CuInX}_2$ ,  $X=\text{S, Se, Te}$ ) and three mixed-cation ( $\text{CuMSe}_2$ ,  $M=\text{Al, Ga, In}$ ) chalcopyrite systems. The random chalcopyrite alloys are represented by special quasirandom structures (SQS). The calculated bowing coefficients are in good agreement with the most recent experimental data for stoichiometric alloys. Results for the mixing enthalpies and the band offsets are provided as predictions to be tested experimentally. Comparing our calculated bowing and band offsets for the mixed-anion chalcopyrite alloys with those of the corresponding Zn chalcogenide alloys ( $\text{ZnX}$ ,  $X=\text{S, Se, Te}$ ), we find that the larger  $p-d$  coupling in chalcopyrite alloys reduces their band offsets and optical bowing. Bowing parameters for ordered, Zn-based II-VI alloys in the CuAu, CuPt, and chalcopyrite structures are presented: we find that ordered  $\text{Zn}_2\text{SeTe}$  has bowing coefficients of 1.44 and 3.15 eV in the CuAu and CuPt structures, while the random  $\text{ZnSe}_x\text{Te}_{1-x}$  alloy has a bowing of 1.14 eV. The band alignment between  $\text{CuInSe}_2$  and  $\text{CuInSe}_2$ -derived ordered vacancy compounds are also presented. © 1995 American Institute of Physics.

## I. INTRODUCTION

$A_{1-x}B_x$  semiconductor alloys constitute a group of technologically important materials since their structural, transport, and optical properties can be tuned continuously by varying the composition  $x$ , thus broadening the range of material properties available from the pure constituents  $A$  and  $B$ . For example, the band gaps  $E_g(x)$  of  $A_{1-x}B_x$  alloys can often be described by

$$E_g(x) = (1-x)E_g(A) + xE_g(B) - bx(1-x), \quad (1)$$

where  $b$  is an "optical bowing coefficient." Figure 1 illustrates that alloys between different I-III-VI<sub>2</sub> chalcopyrites<sup>1-4</sup> offer a new, redshifted range of band gaps relative to the alloys of common II-VI compounds.<sup>5,6</sup> It has been shown recently<sup>7,8</sup> that alloys of  $\text{CuInSe}_2$  with either  $\text{CuGaSe}_2$  or with  $\text{CuInS}_2$  can increase the band gap of  $\text{CuInSe}_2$ , a change that increases the efficiency of thin-film  $\text{CuInSe}_2$  solar cells.<sup>9</sup> In Table I we summarize the measured<sup>10-33</sup> bowing parameters of the Cu-based chalcopyrite alloys, while Table II give analogous results<sup>34-41</sup> for the Zn chalcogenide alloys. Table I illustrates that, while the properties of the end point chalcopyrite materials are known rather well, very little is known definitely about the properties of their alloys. In fact, measurements of optical bowing parameters are lacking for many Cu-III-VI<sub>2</sub> alloys with III=Al, Ga, In and VI=S, Se, Te and, in those cases where data are available, the scatter between different measurements on the same alloy is significant. In some cases, even the sign of the bowing parameter is under dispute, e.g.,  $\text{CuIn(S,Se)}_2$  and  $\text{Cu(Ga,In)Se}_2$ . Other properties, such as the band offsets between the chalcopyrite compounds (needed for device design),<sup>9</sup> are also generally unknown. From the point of view of fundamental physics, it is interesting to understand not only why the absolute band

gaps of individual chalcopyrite compounds are significantly lower than those of the corresponding II-VI compounds [e.g.,  $E_g(\text{CuGaX}_2) < E_g(\text{ZnX})$  for  $X=\text{S, Se, Te}$ ; see Fig. 1]<sup>4</sup> but also why the chalcopyrite bowing parameters (Tables I and II) and valence-band offsets (see below) are systematically smaller than the corresponding values in the zinc-blende counterparts [e.g.,  $b(\text{CuMS}_{1-x}\text{Se}_x) < b(\text{ZnS}_{1-x}\text{Se}_x)$  and  $b(\text{CuMSe}_{1-x}\text{Te}_x) < b(\text{ZnSe}_{1-x}\text{Te}_x)$ ].

In this paper we have calculated the (i) alloy bowing coefficients, (ii) alloy mixing enthalpies, and (iii) valence- and conduction-band lineups at the relaxed interface between mixed-cation  $\text{CuAlSe}_2/\text{CuGaSe}_2/\text{CuInSe}_2$  and mixed-anion  $\text{CuInS}_2/\text{CuInSe}_2/\text{CuInTe}_2$  chalcopyrites. We use first prin-

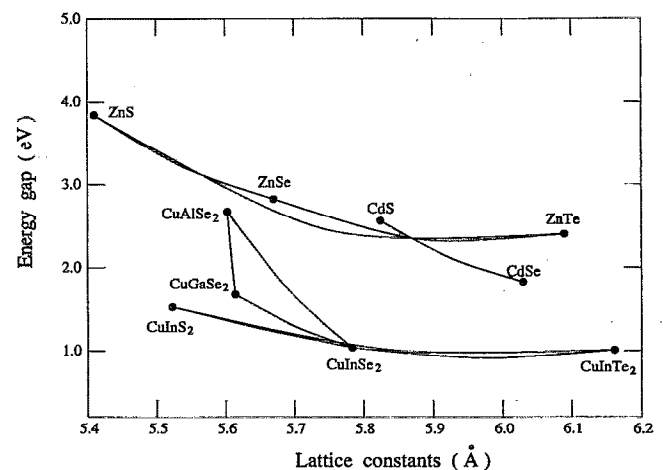


FIG. 1. Energy gap vs lattice constant for some chalcopyrite alloys and II-VI alloys. Our calculated bowing coefficients are used together with Eq. (1) to describe band gaps as a function of composition  $x$ , while for the lattice constant we use Eq. (5). Experimental values (solid dots) are used for the end-point compounds (see Table IV below).

<sup>a)</sup>Electronic mail: shw@nrel.gov

TABLE I. Measured optical bowing parameters  $b$  (in eV) of the lowest gaps in Cu-based single-crystal or polycrystalline chalcopyrite alloys. The values of Samanta *et al.* (Ref. 13) are also given. "single" and "poly" refer to single crystal and polycrystalline, respectively. Blank entries denote absence of data.

System	$b$	Sample type	Growth method	Author (year)	Reference
Mixed anion					
CuAl(S,Se) <sub>2</sub>	0.34	Single	Iodine chemical transport	Shirakata <i>et al.</i> (1994)	Ref. 10
CuGa(S,Se) <sub>2</sub>	-0.01	Single	Iodine chemical transport	Roa <i>et al.</i> (1990)	Ref. 11
	0.00	Single	Iodine chemical transport	Shirakata <i>et al.</i> (1993)	Ref. 12
	0.00			Samanta <i>et al.</i> (1993)	Ref. 13
CuIn(S,Se) <sub>2</sub>	-0.12	Single	Powder mix	Chapman <i>et al.</i> (1979)	Ref. 14
	0.00	Single	Iodine chemical transport	Bodnar <i>et al.</i> (1981)	Ref. 15
	0.02	Single	Melt and anneal	Quintero <i>et al.</i> (1984)	Ref. 16
	0.14	Single	Melt and anneal	Abid <i>et al.</i> (1987)	Ref. 17
	-0.02			Samanta <i>et al.</i> (1993)	Ref. 13
CuAl(Se,Te) <sub>2</sub>					
CuGa(Se,Te) <sub>2</sub>	0.22	Single	Melt and anneal	Avon <i>et al.</i> (1983)	Ref. 18
	0.34	Poly	Melt and anneal	Chatrathorn <i>et al.</i> (1985)	Ref. 19
	0.00			Samanta <i>et al.</i> (1993)	Ref. 13
CuIn(Se,Te) <sub>2</sub>	0.39	Single	Melt and anneal	Avon <i>et al.</i> (1983)	Ref. 18
	0.35	Poly	Melt and anneal	Chatrathorn <i>et al.</i> (1985)	Ref. 19
	0.42	Poly	Melt and anneal	Quintero <i>et al.</i> (1991)	Ref. 20
	0.30			Samanta <i>et al.</i> (1993)	Ref. 13
CuAl(S,Te) <sub>2</sub>					
CuGa(S,Te) <sub>2</sub>	-0.30			Samanta <i>et al.</i> (1993)	Ref. 13
CuIn(S,Te) <sub>2</sub>	1.02	Single	Melt and anneal	Grima <i>et al.</i> (1988)	Ref. 21
Mixed cation					
Cu(Al,Ga)S <sub>2</sub>	0.34	Single	Iodine chemical transport	Tsuboi <i>et al.</i> (1988)	Ref. 22
Cu(Al,Ga)Se <sub>2</sub>	0.28	Single	Iodine chemical transport	Shirakata <i>et al.</i> (1993)	Ref. 23
Cu(Al,Ga)Te <sub>2</sub>					
Cu(Ga,In)S <sub>2</sub>	0.19	Single	Iodine chemical transport	Bodnar <i>et al.</i> (1986)	Ref. 24
	0.31	Single	Iodine chemical transport	Shirakata <i>et al.</i> (1993)	Ref. 12
	0.15			Samanta <i>et al.</i> (1993)	Ref. 13
	0.20			Samanta <i>et al.</i> (1993)	Ref. 13
Cu(Ga,In)Se <sub>2</sub>	0.15	Single	Iodine chemical transport	Bodnar <i>et al.</i> (1982)	Ref. 25
	-0.07	Single	Melt and anneal	Avon <i>et al.</i> (1983)	Ref. 18
	0.03	Single	Melt and anneal	Abid <i>et al.</i> (1987)	Ref. 17
	0.16	Single	Bridgman	Ciszek <i>et al.</i> (1987)	Ref. 26
	0.16	Single	Bridgman	Durran (1987)	Ref. 27
	0.11	Poly	Evaporation	Dimmler <i>et al.</i> (1987)	Ref. 28
	0.14	Poly	Evaporation	Chen <i>et al.</i> (1987)	Ref. 29
	0.24	Poly	Evaporation	Albin <i>et al.</i> (1991)	Ref. 30
	0.15	Single	Chemical vapor deposition	Tinoco <i>et al.</i> (1991)	Ref. 31
	0.13	Poly	RF sputtering	Yamaguchi <i>et al.</i> (1992)	Ref. 32
	0.02	Single	Iodine chemical transport	Larez <i>et al.</i> (1994)	Ref. 33
	0.15			Samanta <i>et al.</i> (1993)	Ref. 13
	0.17			Samanta <i>et al.</i> (1993)	Ref. 13
0.21			Samanta <i>et al.</i> (1993)	Ref. 13	
Cu(Ga,In)Te <sub>2</sub>	-0.22	Single	Melt and anneal	Avon <i>et al.</i> (1983)	Ref. 18
	-0.33			Samanta <i>et al.</i> (1993)	Ref. 13
Cu(Al,In)S <sub>2</sub>					
Cu(Al,In)Se <sub>2</sub>					
Cu(Al,In)Te <sub>2</sub>					

ciples; self-consistent electronic structure theory based on the local density approximation<sup>42</sup> (LDA). Our principal results for the bowing parameters ( $b$ ), the mixing enthalpy at  $x=1/2$  ( $\Delta H$ ) and the valence-band offset ( $\Delta E_v$ ) are summarized in Fig. 2 for mixed-anion chalcopyrites (part a) and mixed-cation chalcopyrites (part b) alloys. Results for mixed-anion Zn chalcogenide alloys are given in Fig. 3. This paper describes how such calculations are done (Sec. II) and discusses the significant physics of the results (Sec. III).

## II. METHOD OF CALCULATION

### A. Special quasirandom structures

A random alloy is distinguished from an ordered compound by the fact that the site occupations in the latter are fixed deterministically by the space group symmetry, while for random alloys the site occupations are known only probabilistically. A direct computational approach to construct a structural model for random substitutional  $A_xB_{1-x}$  alloys is

TABLE II. Measured bowing parameters  $b$  (in eV) of the lowest gaps in Zn-based chalcogenide alloys. "Single" and "poly" refer to single crystal and polycrystalline, respectively.

System	$b$	Sample type	Growth method	Author (year)	Reference
Zn(S,Se)	0.41	Single	Melt and anneal	Suslina <i>et al.</i> (1977)	34
	0.63	Single	Chemical vapor deposition	Ebina <i>et al.</i> (1974)	35
	0.43	Single	Iodine chemical transport	Mach <i>et al.</i> (1982)	36
	0.55	Poly	Evaporation	Shazly <i>et al.</i> (1985)	37
Zn(Se,Te)	1.23	Single	Chemical vapor deposition	Ebina <i>et al.</i> (1972)	38
	1.51		molecular beam epitaxy	Brasil <i>et al.</i> (1991)	39
Zn(S,Te)	3.0	Poly	Evaporation	Hill <i>et al.</i> (1973)	40
	3.2		molecular beam epitaxy	Wong <i>et al.</i> (1994)	41

to consider a huge unit cell whose sites are occupied by  $A$  and  $B$  according to a given probability distribution. Applying (for mathematical convenience) periodic boundary conditions then gives a "pseudo-ordered crystal" that can be treated theoretically by standard band structure methods. For sufficiently large "supercells" this approach becomes exact. In practice, this approach has been applied within the context of semiempirical electronic structure methods for  $\sim 2000$  atom/cell, producing rather accurate results.<sup>43-45</sup> Despite the success of this direct method, this procedure requires a large number of atoms to attain statistical significance, thus is not

computationally practical in conjunction with the highly accurate but mathematically complex first-principles LDA band-structure methods. There is, however, a more efficient way to achieve practically the same result: we know that the physical properties of an alloy are uniquely determined by its atomic structure, and that the structure can be quantified by the "structural correlation functions"  $\bar{\Pi}_{k,m}$  for atomic clusters  $(k,m)$  with  $k$  vertices and up to  $m$ th neighbor.<sup>46</sup> Hence, rather than occupy sites of a huge unit cell *at random*, one can occupy sites of a "small" unit cell (the "special quasirandom structures," or SQS<sup>47</sup>) by  $A$  and  $B$  atoms so that its physically most relevant structural correlation functions  $\bar{\Pi}_{k,m}$  are forced to be closest to the exact values in an infinite random alloy [ $\bar{\Pi}_{k,m} = (2x - 1)^k$ ]. This yields rather small supercells ( $\sim 20$  atoms) with correlation functions that approach the exact values in very large random supercells.

The SQS method has been previously applied to III-V<sup>45,47,48</sup> and II-VI<sup>47,49</sup> zinc-blende alloys as well as to fcc transition metal alloys.<sup>50,51</sup> The coordinates of these SQS can be found in these references (a more detailed description and a list of the SQS coordinates for zinc-blende alloys can be obtained from the FTP site <ftp://ftp.nrel.gov/pub/sst/archive/sqs>). Here we apply the SQS method to alloys between chalcopyrites.

For mixed-anion chalcopyrite alloys [e.g.,  $\text{CuIn}(\text{S}_{0.5}\text{Se}_{0.5})_2$ ], the anions occupy an fcc sublattice, hence, for the anion sublattice we can use the fcc SQS. The cation

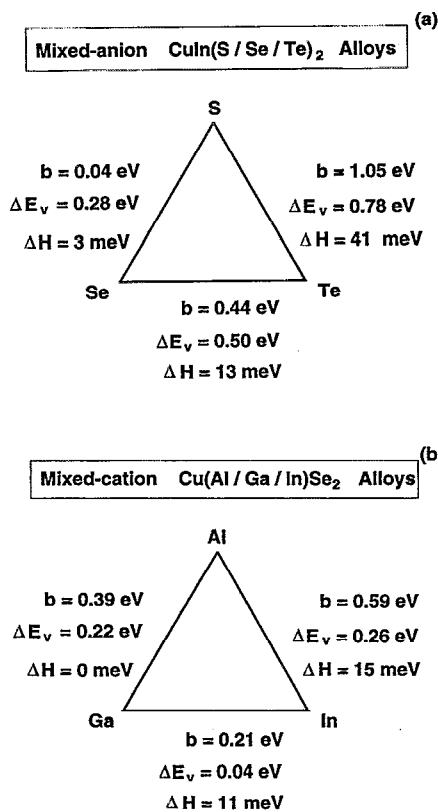


FIG. 2. Calculated bowing coefficients  $b$ , valence-band offsets  $\Delta E_v$ , and alloy mixing energies  $\Delta H$  at  $x=1/2$  of (a) mixed-anion chalcopyrite alloys and (b) mixed-cation chalcopyrite alloys.  $\Delta H$  is given in meV per atom. The value given in the figure should be multiplied by two to convert it to meV per mixed-atom for mixed-anion alloys. For mixed-cation alloys the value should be multiplied by four.

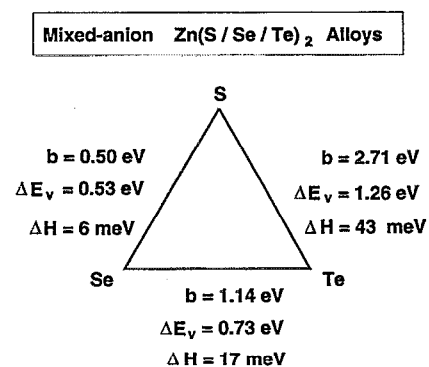


FIG. 3. Calculated bowing coefficients  $b$ , valence-band offsets  $\Delta E_v$ , and alloy mixing energies  $\Delta H$  at  $x=1/2$  of mixed-anion chalcogenide alloys.  $\Delta H$  is given in meV per atom. The value given in the figure should be multiplied by two to convert it to meV per *mixed-atom*.

TABLE III. Structural correlation functions  $\bar{\Pi}_{k,m}$  of the random alloys at  $x=1/2$ , where  $k$  is the number of vertices of the cluster ( $k=2$  is pair,  $k=3$  is three-body, etc.) and  $m$  is the separation ( $m=1,2$  are first and second neighbors, respectively). For the mixed-cation SQS we use the notation of fcc clusters. A non-zero value of a correlation function of the SQS implies deviation from perfect randomness.

Name	$\bar{\Pi}_{1,1}$	$\bar{\Pi}_{2,1}$	$\bar{\Pi}_{3,1}$	$\bar{\Pi}_{4,1}$	$\bar{\Pi}_{2,2}$	$\bar{\Pi}_{2,3}$	$\bar{\Pi}_{2,4}$	$\bar{\Pi}_{2,5}$
SQS (mixed cation)	0	0			-2/3	0	1/3	0
SQS (mixed anion)	0	0	0	-1	-1/3	0	-1/3	0
Exact random	0	0	0	0	0	0	0	0

sublattice needs to have the chalcopyrite translational symmetry, so that the final SQS unit cell should be commensurate with both the chalcopyrite structure of the cation sublattice and with the SQS of the anion sublattice. This is achieved here using a sixteen atom SQS unit cell. It has the Cartesian lattice vectors:

$$\begin{aligned} \mathbf{a}_1 &= (1, -1, 2\eta) \frac{a}{2}; & \mathbf{a}_2 &= (-1, 1, 2\eta) \frac{a}{2}; \\ \mathbf{a}_3 &= (2, 2, 0) \frac{a}{2}, \end{aligned} \quad (2)$$

where  $a$  is the lattice constant and  $\eta=c/2a \sim 1$  is the tetragonal ratio. In this unit cell the anions form an fcc SQS4 (an  $A_2B_2$  superlattice along the [110] direction).<sup>49</sup>

For Cu-based *mixed-cation chalcopyrite alloys* (e.g.,  $\text{CuGa}_{0.5}\text{In}_{0.5}\text{Se}_2$ ) the mixed-cation atoms occupy a body centered tetragonal lattice. The Cu sublattice has the chalcopyrite translational symmetry, while the anions occupy an fcc sublattice. In the present calculation, we used a 16-atom SQS cell (with four mixed atoms) which has the same lattice vectors as in Eq. (2). For unrelaxed  $\text{CuGa}_{0.5}\text{In}_{0.5}\text{Se}_2$  alloy the eight cations are located at

$$\begin{aligned} \text{Cu}^{(1)}(0,0,0) \frac{a}{2}; & \quad \text{Cu}^{(2)}(0,1,1) \frac{a}{2}, \\ \text{Cu}^{(3)}(1,1,2) \frac{a}{2}; & \quad \text{Cu}^{(4)}(2,1,1) \frac{a}{2}, \\ \text{Ga}^{(1)}(0,0,2) \frac{a}{2}; & \quad \text{Ga}^{(2)}(1,0,1) \frac{a}{2}, \\ \text{In}^{(1)}(1,1,0) \frac{a}{2}; & \quad \text{In}^{(2)}(1,2,1) \frac{a}{2}. \end{aligned} \quad (3)$$

It is interesting to see that the mixed cations also form an  $A_2B_2$  superlattice along the [110] direction. The structural correlation functions of these SQS are given in Table III; they are compared with the ideal random alloy correlation functions. We see that for both mixed-cation and mixed-anion alloys the first error of pair correlation functions occurs at the second neighbor. For mixed anion, an error also occurs in the first-neighbor four-body correlation functions.

## B. Relaxing interatomic distances in the alloy

A pure  $ABX_2$  chalcopyrite has two nearest-neighbor cation-anion bonds with lengths given by

TABLE IV. Structural parameters and band gaps used in the present calculation for five pure chalcopyrite compounds and three Zn-based II-VI compounds. The experimental data given in Refs. 2 and 4 are used for chalcopyrite compounds, except for  $\text{CuAlSe}_2$  where we used our estimated internal relaxation parameter  $u=0.259$ . The experimental data for Zn compounds are from Ref. 5. Our calculated LDA crystal field splitting  $\Delta_{\text{CF}}$  and spin-orbit splitting  $\Delta_{\text{SO}}$  for these compounds are given in the last two columns.

System	$a$ (Å)	$\eta=c/a$	$u$	$E_g$ (eV)	$\Delta_{\text{SO}}$ (eV)	$\Delta_{\text{CF}}$ (eV)
$\text{CuInS}_2$	5.523	1.007	0.214	1.53	-0.02	-0.00
$\text{CuInSe}_2$	5.784	1.004	0.224	1.04	0.184	-0.02
$\text{CuAlSe}_2$	5.602	0.977	0.259	2.67	0.152	-0.16
$\text{CuGaSe}_2$	5.614	0.982	0.250	1.68	0.194	-0.12
$\text{CuInTe}_2$	6.161	1.003	0.225	1.01	0.598	-0.00
ZnS	5.409	1.000	0.250	3.84	0.068	0.000
ZnSe	5.668	1.000	0.250	2.82	0.396	0.000
ZnTe	6.089	1.000	0.250	2.40	0.883	0.000

$$\begin{aligned} R_{AX} &= a \left[ \frac{1}{16} + u^2 + \frac{\eta^2}{16} \right]^{1/2}, \\ R_{BX} &= a \left[ \frac{1}{16} + \left( \frac{1}{2} - u \right)^2 + \frac{\eta^2}{16} \right]^{1/2}, \end{aligned} \quad (4)$$

where  $a$  is the lattice constant,  $\eta=c/2a$  is the tetragonal ratio, and  $u$  is a dimensionless internal relaxation parameter. In the undistorted lattice  $u=1/4$  and  $\eta=1$ , so  $R_{AX}=R_{BX}=(\sqrt{3}/4)a$ . In a *pure* chalcopyrite crystal the structure is determined once  $\{a, \eta, u\}$  are specified. In a chalcopyrite *alloy*, however, there are many more internal and external structural parameters that need to be determined. It is crucial to find the equilibrium values of these parameters since band gaps depend on atomic relaxation.<sup>4</sup> Our first-principles total energy and force calculations show that for these rather ionic alloys the anion-cation bond lengths have almost the same values as in the pure chalcopyrite constituents. This principle of ‘‘conservation of tetrahedral bond lengths’’<sup>4</sup> indicates that the bond bending force<sup>52,53</sup> in chalcopyrites is rather small. Hence, we have determined the relaxed atomic positions in our chalcopyrite SQS and superlattices of  $(ABX_2)_n/(A'B'X'_2)_n$  (Sec. II D) by requiring that (i) the nearest-neighbor anion-cation bond lengths in the alloy equal their respective values in the pure chalcopyrite compounds and that (ii) the lattice constant is given by Vegard’s rule<sup>54</sup>

$$a(x) = (1-x)a_{ABX_2} + xa_{A'B'X'_2}. \quad (5)$$

These requirements uniquely determine all cell-internal and cell-external parameters of the model alloy.

The input<sup>2,4</sup>  $\{a, u, \eta\}$  to our calculation is given in the first three columns of Table IV. Using these values for each chalcopyrite and Eq. (4) we determine the bond lengths in the *alloy*. In all cases but  $\text{CuAlSe}_2$  we use measured values.<sup>2,4</sup> In  $\text{CuAlSe}_2$  we use  $u=0.259$  rather than the value of 0.269 given in Ref. 55. This is based on our total energy calculation and on the observation that the Cu–Se bond lengths in the three Se-based chalcopyrite compounds  $\text{CuMSe}_2$  (Table IV) should be similar. It is interesting to notice that in the more covalent III-V compounds ( $V=\text{P, As, Sb}$ ) the Al–V bond length is slightly *longer*<sup>6</sup> (by 0.1%–

0.6%) than the Ga–V bond length, while in the ionic nitrides the Al–N bond length is about 3% shorter than the Ga–N bond length.<sup>6</sup> Using the value in Table IV for the ionic chalcopyrite, we find that the Al–Se bond length is about 2% smaller than the Ga–Se bond. The difference between the In bond length and the Ga bond length are found to be similar in III–V’s and in chalcopyrites.

### C. Calculation of band structure and total energy

Using the unit cell structure of the SQS (Sec. II A) and the relaxed atomic positions (Sec. II B) we can now apply band-structure techniques to evaluate the alloy band gaps  $E_g$  and total energy  $E_{\text{tot}}$ . The band-structure calculations were performed using the density functional formalism as implemented by the general potential, relativistic, all electron, linearized augmented plane wave (LAPW) method.<sup>56</sup> [Note that the earlier calculations of Jaffe and Zunger<sup>3,4</sup> were nonrelativistic.] We used the Ceperley–Alder exchange correlation potential<sup>57</sup> as parameterized by Perdew and Zunger.<sup>58</sup> The Brillouin zone integration of the superstructures is performed using special  $\mathbf{k}$  points which are equivalent<sup>59</sup> to the ten special  $\mathbf{k}$  points in the zinc-blende Brillouin zone. Table IV shows our calculated spin-orbit splitting  $\Delta_{\text{SO}}$  and crystal-field splitting  $\Delta_{\text{CF}}$  at the valence-band maximum (VBM) for five pure chalcopyrite and for the Zn chalcogenides.

The crystal-field splitting  $\Delta_{\text{CF}} = \epsilon(\Gamma_{5v}) - \epsilon(\Gamma_{4v})$  is calculated by turning off the spin-orbit interaction. We find that for all the chalcopyrites studied here the crystal-field splittings  $\Delta_{\text{CF}}$  are negative, and become even more negative as the tetragonal distortion  $1 - \eta$  increases.<sup>1</sup> This explains the fact that  $\text{CuAlSe}_2$  and  $\text{CuGaSe}_2$  have large negative  $\Delta_{\text{CF}}$ . Our calculated  $\Delta_{\text{CF}}$  are in good agreement with experimental data.<sup>10,22,32</sup>

The spin-orbit splittings are obtained by fitting the calculated fully relativistic band energies to the quasicubic model of Hopfield.<sup>60</sup> We see from Table IV that the spin-orbit splittings of the chalcopyrites are much smaller than the corresponding values in the II–VI Zn compounds. For  $\text{CuInS}_2$ ,  $\Delta_{\text{SO}}$  is even slightly negative. This is because in chalcopyrites the Cu 3*d* energy level is much closer to the anion *p*-like VBM than is the Zn 3*d* level to its VBM in Zn chalcogenides.<sup>3,61</sup> Hence, *p*–*d* repulsion and mixing are stronger in the chalcopyrites. Since *d* orbitals contribute a negative term to the spin-orbit splitting,<sup>62–64</sup> the larger mixing of the cation *d* orbital in chalcopyrites produces a reduction of the spin-orbit splitting relative to II–VIs. This stronger repulsion in chalcopyrites is also responsible for the smaller band gaps<sup>3,4</sup> relative to their corresponding II–VI compounds (Table IV and Fig. 1).

### D. Calculation of band offsets

To calculate the valence-band offset  $\Delta E_v(ABX_2/A'B'X'_2)$  at the interface between two chalcopyrites  $ABX_2$  and  $A'B'X'_2$  we follow the procedure<sup>65</sup> used in photoemission core-level spectroscopy, where the band offset is given by

$$\Delta E_v = \Delta E_{\text{VBM},C}^{ABX_2} - \Delta E_{\text{VBM}',C'}^{A'B'X'_2} + \Delta E_{C,C'} \quad (6)$$

Here,

$$\Delta E_{\text{VBM},C}^{ABX_2} = E_{\text{VBM}}^{ABX_2} - E_C^{ABX_2} \quad (7)$$

and

$$\Delta E_{\text{VBM}',C'}^{A'B'X'_2} = E_{\text{VBM}'}^{A'B'X'_2} - E_{C'}^{A'B'X'_2} \quad (8)$$

are the core level to valence-band maximum energy separations for  $ABX_2$  and  $A'B'X'_2$ , respectively, and

$$\Delta E_{C,C'} = E_C^{ABX_2} - E_{C'}^{A'B'X'_2} \quad (9)$$

is the difference in core-level binding energy between  $ABX_2$  and  $A'B'X'_2$  on each side of the interface. In our calculation, the core-to-VBM energy difference  $\Delta E_{\text{VBM},C}$  is obtained as an eigenvalue difference for each of the component chalcopyrites. We wish to obtain the band offset for a fully relaxed interface, where each component has its own equilibrium lattice parameter. Thus, the first two terms in Eq. (6) are calculated at their respective equilibrium structural parameters appropriate to the isolated compound (Table IV). The core-level difference  $\Delta E_{C,C'}$  between the two chalcopyrites is obtained from the calculation for the  $(ABX_2)_n/(A'B'X'_2)_n$  superlattices with (001) orientation. The superlattice layer thickness  $n$  is increased until the core levels of the innermost layer on each side of the superlattice are bulk like. We find that for  $n=2$  the uncertainty due to the choice of different core levels is about 0.05 eV. The structural parameters of the superlattice are determined using the description of Sec. II B. The resulting structure does not correspond to relaxed constituents; the small core level shift due to strain<sup>66</sup> is neglected. If one is interested in the case where the chalcopyrites form a coherently strained interface, the band edge energy of each chalcopyrite needs to be shifted relative to the results of this paper. The shift depends on the size and direction of the strain through the deformation potential.<sup>67</sup> These shifts should be added to the first two terms of Eq. (6),<sup>68</sup> while the shift in the third term is expected to be small.<sup>66</sup>

## III. RESULTS

### A. Mixing enthalpy

The mixing enthalpy of the random chalcopyrite alloy<sup>6</sup> can be obtained from the calculated alloy total energies as

$$\Delta H(x=1/2) = E_{\text{tot}}(ABX_2/A'B'X'_2) - E_{\text{tot}}(ABX_2) - E_{\text{tot}}(A'B'X'_2) \quad (10)$$

Our calculated results are denoted as  $\Delta H$  in Fig. 2. We find that for both mixed-anion and mixed-cation alloys the mixing enthalpy is positive and increases as the lattice mismatch increases. For example,  $\Delta H(\text{S,Se})$ ,  $\Delta H(\text{Se,Te})$ , and  $\Delta H(\text{S,Te})$  are 3, 13, and 41 meV/atom, respectively, while the size-mismatches  $\Delta a/\bar{a}$  are 4.6%, 6.3%, and 10.9%, respectively. The positive sign of  $\Delta H$  indicates that here, the ground state at  $T=0$  corresponds to phase separation into the pure chalcopyrite constituents. (However, at finite temperatures, the disordered phase can be stabilized through entropy.) The mixing enthalpy  $\Delta H$  is rather small for (S,Se)

### Relaxed Chalcopyrite Superlattices

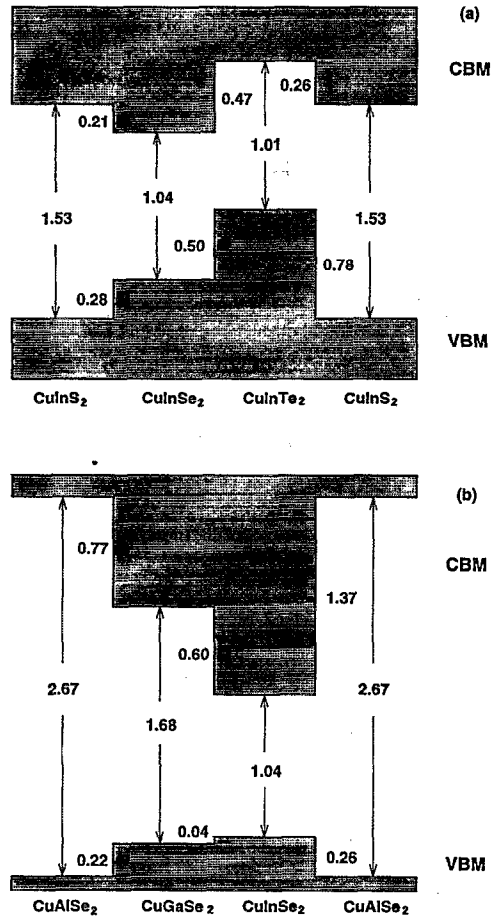


FIG. 4. Calculated intrinsic valence-band and conduction-band offsets for interfaces between (a) common-cation chalcopyrite compounds and (b) common-anion chalcopyrite compounds. The values pertain to fully relaxed components having their free-space equilibrium structures.

and (Al,Ga) chalcopyrite alloys, and is slightly larger for (Se,Te), (Ga,In), and (Al,In) alloys. The rather small values of  $\Delta H$  for the (S,Se), (Al,Ga), (Se,Te), and (Ga,In) alloys suggest that they will be miscible in the whole composition range at finite temperatures. The mixing enthalpy  $\Delta H$  is large for the (S,Te) alloy, suggesting that large miscibility gap can exist in this system.<sup>16</sup>

We have also calculated the mixing enthalpy for mixed-anion Zn-based II-VI alloys Zn(S,Se), Zn(Se,Te), and Zn(S,Te). For these Zn alloys the equilibrium structural parameters are determined using the valence force field (VFF) model.<sup>52,53</sup> We find that the mixed-anion chalcopyrite alloys [Fig. 2(a)] have smaller mixing enthalpies than the corresponding Zn alloys (Fig. 3). This is consistent with the observation that the chemical disparity between the alloyed elements is reduced in chalcopyrites relative to the II-VI alloys (see Secs. III B and III E below) and that chalcopyrites have smaller bond bending force constants, thus, smaller elastic strain energies.

### Relaxed Zn-Based II-VI Superlattices

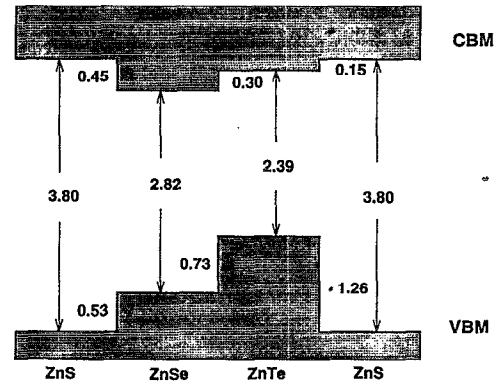


FIG. 5. Calculated intrinsic valence-band and conduction-band offsets for interfaces between Zn-based II-VIs. The values pertain to fully relaxed components having their free-space equilibrium structures.

## B. Band offsets

Using the procedure described in Sec. II D we have calculated the intrinsic valence-band offsets between the three common-cation CuInS<sub>2</sub>/CuInSe<sub>2</sub>/CuInTe<sub>2</sub> chalcopyrites [Fig. 4(a)], and between the three common-anion CuAlSe<sub>2</sub>/CuGaSe<sub>2</sub>/CuInSe<sub>2</sub> chalcopyrites [Fig. 4(b)]. For comparison, we have also calculated the intrinsic valence-band offsets between the II-VI ZnS/ZnSe/ZnTe chalcogenides (Fig. 5). The conduction band offsets  $\Delta E_c$  are obtained using the relation

$$\Delta E_c = \Delta E_g - \Delta E_v, \quad (11)$$

where  $\Delta E_g$  is the *measured*<sup>4</sup> band gap (Table IV) difference between the compounds. We find the following results:

(i) The S/Se band lineup is “type I,” while the Se/Te band lineup is “type II.” This is true both in II-VIs and in chalcopyrites. For the S/Te interface, the lineup is type II in chalcopyrites and type I in II-VIs. However, strain may change the type of the lineup (see below). For the mixed-cation chalcopyrites, the lineup is always type I.

(ii) For common-cation chalcopyrites [Fig. 4(a)] the band offsets are large both in the valence band and in the conduction band. The large valence-band offsets are consistent with the fact that the VBM is anion *p*-like state, and that the valence-band offsets for these systems mainly reflect the differences between anion *p* orbital energies. The atomic *p* orbital energies increase from S to Se to Te (Table V). The large conduction-band offset is partly due to the anion *s* orbital energy differences (Table V) and partly due to the fact that the CBM energy moves up as the volume of the compound decreases.

(iii) The valence band offsets between common-cation chalcopyrite system are smaller than those between the corresponding II-VIs (Fig. 5). The reason is the larger *p*-*d* repulsion in chalcopyrites: the *p*-*d* repulsion is inversely proportional to the energy difference between the cation *d* and anion *p* state.<sup>63,64,69</sup> In the chalcopyrite and II-VI compounds the cation *d* bands are below the anion *p* bands.<sup>3</sup> Thus, the deeper the anion *p* level is, the closer it is to the

TABLE V. Calculated (semirelativistic) atomic LDA valence orbital energies  $\epsilon_s$ ,  $\epsilon_p$ , and  $\epsilon_d$  (in eV) of the elements studied in this paper.

Atom	$\epsilon_s$	$\epsilon_p$	$\epsilon_d$
S	-17.36	-7.19	
Se	-17.56	-6.74	
Te	-15.43	-6.19	
Al	-7.91	-2.86	
Ga	-9.25	-2.82	-19.18
In	-8.56	-2.77	-18.75
Cu	-4.95		-5.39
Zn	-6.31	-1.31	-10.49

Cu  $d$  level. Since the  $p$  orbital energy decreases from Te to Se to S, the  $p-d$  repulsion is stronger in sulphides than in selenides and tellurides, and the upward shift of the VBM is larger in sulphides than in selenides and tellurides. Therefore,  $p-d$  repulsion diminishes the difference between anion  $p$  orbitals and thus the valence-band offset. This effect is weaker in II-VI systems than in the chalcopyrite systems, since the Cu  $3d$  in the chalcopyrites is much closer to the VBM than the Zn  $3d$  in Zn compound, so the reduction of the band offset due to the  $p-d$  repulsion is larger in the chalcopyrite systems.

(iv) For common-anion chalcopyrites [Fig. 4(b)] we find that most of the band offset is in the conduction band. The valence-band offset is small, indicating that the common-anion rule<sup>70</sup> (which states that since the VBM is primarily a bonding anion  $p$  state, the valence-band offset for the common-anion system should be small) is followed rather well for this system. Although this rule holds in some cases (e.g., GaV/InV,  $\Delta E_v \sim 0.1$  eV), it does not hold in other cases (e.g., AlV/GaV and AlV/InV, where the band offset  $\Delta E_v \sim 0.5$  eV for  $V=P, As, \text{ and } Sb$ ).<sup>71</sup> The breakdown of the common-anion rule in zinc-blende systems (e.g., AlAs/GaAs) is attributed<sup>62-64</sup> to the coupling between anion  $p$  and cation  $d$  orbitals. For GaAs the cation  $d$  bands are below the anion  $p$  bands, hence  $p-d$  repulsion pushes the VBM up. On the other hand, in AlAs the empty cation  $d$  bands are above the anion  $p$  bands, hence  $p-d$  repulsion pushes the VBM down. Thus, the VBM of GaAs is higher in energy than AlAs. The same  $p-d$  coupling effect exists in the Cu-based chalcopyrite compounds. However, in chalcopyrites half of the cation sublattice is occupied by Cu atoms and these atoms occur equally on both sides of the interface. One thus expects that the valence band offset in chalcopyrites will be about half the values in the corresponding III-V system.

(v) We find that for both common-cation and common-anion chalcopyrite interfaces, the transitivity rule<sup>72</sup> holds for the intrinsic band offsets [i.e.,  $\Delta E_v(A/B) = \Delta E_v(A/C) + \Delta E_v(C/B)$ ]. Assuming that this transitivity rule also holds for an interface between a II-VI compound and a chalcopyrite compound, our present results can be combined with our earlier studies<sup>65,69</sup> of the band offsets between CuInSe<sub>2</sub> and II-VI (CdS and ZnSe) to predict other band offsets between a chalcopyrite compound and a II-VI compound. For example, our calculated<sup>69</sup>  $\Delta E_v$  between CuInSe<sub>2</sub> and CdS is 1.07 eV, hence we expect that  $\Delta E_v$  between CuGaSe<sub>2</sub> and CdS should be 1.03 eV and that  $\Delta E_v$

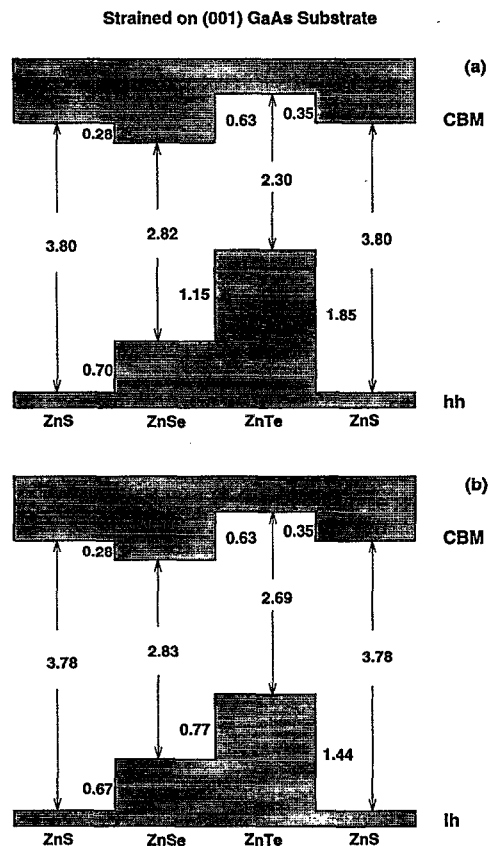


FIG. 6. Calculated valence-band and conduction-band offsets between Zn-based II-VIs strained on a GaAs(001) substrate: (a) lineups for hh states and (b) for lh hole states.

between CuInS<sub>2</sub> and CdS should be 0.79 eV. In some cases (e.g., CuIn<sub>x</sub>Ga<sub>1-x</sub>Se<sub>2</sub>) one may also assume that the VBM of the chalcopyrite alloy is a linear function of composition  $x$ , hence one can estimate the band offset between a chalcopyrite alloy and a II-VI compound.

(vi) Using the pseudopotential method, Nakayama<sup>73</sup> has recently calculated the heavy-hole (hh) valence-band offsets  $\Delta E_{v,hh}$  between different Zn-based II-VI semiconductors strained on a GaAs(001) substrate. He found that  $\Delta E_{v,hh}$  between ZnS/ZnSe, ZnSe/ZnTe, and ZnS/ZnTe are 0.86, 1.29, and 2.15 eV, respectively. These values are larger than our calculated intrinsic band offset of 0.53, 0.73, and 1.26 eV (Fig. 5) obtained for the relaxed interface. The larger values of Nakayama are partly due to strain. To compare our all-electron results with the (no- $d$ ) pseudopotential results of Nakayama, we have calculated directly the valence-band offsets of the strained superlattice using the procedure described in Sec. II D. For a GaAs(001) substrate, our results are shown in Fig. 6 for both hh (part a) and light-hole (lh; part b) band lineups between the strained Zn-based II-VI semiconductors. The hh and lh levels are degenerate for relaxed compounds. For the hh lineup, our calculated  $\Delta E_{v,hh}$  for ZnS/ZnSe, ZnSe/ZnTe, and ZnS/ZnTe are 0.70, 1.15, and 1.85 eV, respectively. These are 0.16, 0.14, and 0.30 eV smaller than Nakayama's values.<sup>73</sup>  $\Delta E_{v,hh}$  increases relative to the relaxed superlattices, since the hh energy increases

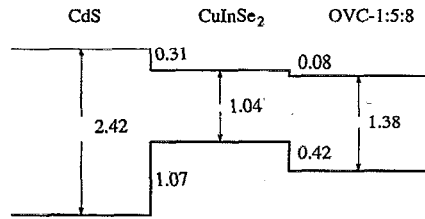


FIG. 7. Calculated valence-band and conduction-band offsets between CdS, CuInSe<sub>2</sub>, and CuIn<sub>5</sub>Se<sub>8</sub> (OVC—1:5:8). Energy is in eV.

almost linearly with the epitaxial strain along the (001) direction.<sup>67</sup> It is interesting to see that for the ZnS/ZnTe interface, the system changes from type I for a relaxed interface (Fig. 5) to type II for a strained interface [Fig. 6(a)]. This is because under strain the CBM energy of ZnTe increases, while that of ZnS decreases. Our calculated  $\Delta E_c$  are given in Fig. 6. The band gap of the compounds also changes with strain, e.g., we find that for the strained ZnTe compound, the band gap is reduced by 0.09 eV. (Note, however, that Nakayama used band gaps for relaxed bulk compounds rather than epitaxially strained values to derive the conduction-band offsets. This can cause errors in his calculation of  $\Delta E_c$ .)

(vii) There are a few indirectly measured values of  $\Delta E_v$ (ZnSe/ZnTe): (a) Based on fitting the dominant photoluminescence peaks to the ZnSe<sub>x</sub>Te<sub>1-x</sub>/ZnTe superlattice band structure obtained by  $k \cdot p$  theory, Rajakarunanyake *et al.*<sup>74</sup> deduced a value for the unstrained valence-band offset  $\Delta E_v$ (ZnSe/ZnTe)=0.91±0.12 eV. This fitting assumed that the observed peak energy corresponds to band edges transition. If the photoluminescence originates instead from (below-the-band-edge) exciton-like transition, the fitted valence-band offset would have been 0.10–0.15 eV smaller.<sup>74</sup> (b) Recently, capacitance-voltage measurement by Ukita *et al.*<sup>75</sup> of a Schottky-like heterojunction barrier gave  $\Delta E_v$ (ZnSe/ZnTe)=0.7–0.8 eV. Both experimental results<sup>74,75</sup> agree very well with our calculated value of 0.73 eV (Fig. 5). However, recent pseudopotential calculation of Freytag<sup>76</sup> treating the Zn 3d states as frozen core found a much larger value of the band offset  $\Delta E_v$ (ZnSe/ZnTe)=1.09 eV. This discrepancy in the band offset between our all-electron calculation and the pseudopotential calculation may be due to the neglect of explicit  $p-d$  coupling in the latter. Recall that  $p-d$  repulsion raises the energy of VBM in inverse proportion to the  $p-d$  energy difference. The effect is thus larger for ZnSe than for ZnTe, so  $p-d$  coupling lowers  $\Delta E_v$ (ZnSe/ZnTe).

(viii) Recently, Schmid *et al.*<sup>77</sup> found that between the CdS and CuInSe<sub>2</sub> layers in CdS/CuInSe<sub>2</sub> solar cells there exists a CuInSe<sub>2</sub>-derived Cu-poor “ordered vacancy compound” (OVC). We have studied<sup>78</sup> the band alignment between CuInSe<sub>2</sub> and the OVC CuIn<sub>5</sub>Se<sub>8</sub>. Our calculated band alignment is given in Fig. 7. Our previous results<sup>69</sup> for the CdS/CuInSe<sub>2</sub> interface are also included in Fig. 7 for comparison. We find from our calculation that the unstrained VBM of CuInSe<sub>2</sub> is 0.42 eV higher than that of CuIn<sub>5</sub>Se<sub>8</sub>. This is due to stronger  $p-d$  coupling in the former. The

TABLE VI. Calculated and the *most reliable* experimental (see references in Table I) values of bowing parameters (in eV) for three mixed-cation and three mixed-anion chalcopyrite alloys. The predictions of Tinoco *et al.* are also given for comparison.

Alloy	Calculated	Experiment	Tinoco <i>et al.</i> <sup>a</sup>
Cu(Al,Ga)Se <sub>2</sub>	0.39	0.28	0.06
Cu(Ga,In)Se <sub>2</sub>	0.21	0.15–0.24	0.18
Cu(Al,In)Se <sub>2</sub>	0.59	...	0.24
CuIn(S,Se) <sub>2</sub>	0.04	~0.0	0.10
CuIn(Se,Te) <sub>2</sub>	0.44	~0.4	0.40
CuIn(S,Te) <sub>2</sub>	1.05	1.02	0.50

<sup>a</sup>Ref. 80.

calculated band gap of CuIn<sub>5</sub>Se<sub>8</sub> is 0.34 eV larger than for CuInSe<sub>2</sub>, so the CBM of CuIn<sub>5</sub>Se<sub>8</sub> is 0.08 eV lower than for CuInSe<sub>2</sub>. We find that many other charge-compensated OVCs can be formally written as an alloy in the form (CuIn<sub>5</sub>Se<sub>8</sub>)<sub>1-x</sub>(Cu<sub>4</sub>In<sub>4</sub>Se<sub>8</sub>)<sub>x</sub>. Hence, the band alignment between any of these OVCs and CuInSe<sub>2</sub> can be linearly interpolated from the values given in Fig. 7. For instance, for the OVC CuIn<sub>3</sub>Se<sub>5</sub> ( $x=0.2$ ), we estimate that its VBM and CBM are 0.34 and 0.06 eV lower than CuInSe<sub>2</sub>, respectively.

### C. Bowing in chalcopyrite alloys

The optical bowing parameter  $b$  of the chalcopyrite alloy is given by

$$b = -4 \left[ E_g(ABX_2/A'B'X'_2) - \frac{1}{2} E_g(ABX_2) - \frac{1}{2} E_g(A'B'X'_2) \right]. \quad (12)$$

Note that both computational and LDA errors<sup>79</sup> tend to cancel in Eqs. (10) and (12), since we compare chemically identical systems in two different forms: the  $ABX_2/A'B'X'_2$  alloys vs. equivalent amounts of the constituents  $ABX_2$  and  $A'B'X'_2$ . Figure 2 gives the calculated bowing parameter for stoichiometric mixed-anion [Fig. 2(a)] and mixed-cation [Fig. 2(b)] chalcopyrite alloys. Comparing our calculated results with the *most reliable* experimental data (see references in Table I) shows good agreement, as illustrated in Table VI.

We next comment on the *experimental* results, so as to decide with what data to compare our calculations. The experimental results of Avon *et al.*,<sup>18</sup> yielding *negative* bowing for Cu(Ga,In)Se<sub>2</sub> and Cu(Ga,In)Te<sub>2</sub>, appear at odds with more recent results. The results of Abid *et al.*<sup>17</sup> for CuIn(S,Se)<sub>2</sub> and Cu(Ga,In)Se<sub>2</sub> are also in disagreement with other measurements. Samanta *et al.*<sup>13</sup> have recently presented bowing parameters for eight chalcopyrite alloys (Table I). We see that some of their results, yielding zero and even *negative* bowing for CuGa(Se,Te)<sub>2</sub> and Cu(Ga,In)Te<sub>2</sub>, seem to be unreasonable. Chatrathorn *et al.*<sup>19</sup> and Quintero *et al.*<sup>20</sup> suggested that bowing for mixed-cation alloys is small<sup>19</sup> ( $b < 0.05$  eV). This is not supported by other experimental measurements and by our calculation. The large scattering of the experimental data (Table I) could reflect

nonstoichiometry<sup>30</sup> in the samples. Table VI collects the measured bowing parameters that we assess as being the most reasonable at this time.

To fit the experimental data for optical bowing of chalcopyrite alloys in which  $A$  and  $B$  are the mixed atoms, Tinoco *et al.*<sup>80</sup> suggested the phenomenological relation

$$b(A,B) = 5/4 |\chi_A - \chi_B|, \quad (13)$$

where  $\chi_\alpha$  is Phillip's electronegativity<sup>81</sup> for atom  $\alpha$ . Their results are also listed in Table VI for comparison. Although their formula correctly gives the bowing coefficients for alloys used in their fitting [(Ga,In), (S,Se), and (Se,Te)], this formula underestimates the bowing of the *other* alloy systems (Al,Ga), (Al,In), and (S,Te). For example, their predicted 0.1 eV increase between  $b(\text{Se,Te})$  and  $b(\text{S,Te})$  is much too small relative to what experiment<sup>16,21</sup> and theory give (0.6 eV). This suggests that the formula of Tinoco *et al.* cannot be reliably extended to systems not used in their fitting. Furthermore, the phenomenological scaling of Eq. (13) does not clarify the physical *mechanism* responsible for bowing, nor does it explain the different bowing of chalcopyrites [e.g., CuGa(S,Se)] versus zinc-blende [Zn(S,Se)] alloys. This will be discussed in Sec. III E below.

#### D. Bowing in Zn-based II-VI alloys

To help understand the physical mechanism controlling the optical bowing, we have calculated the bowing coefficient for Zn-based II-VI alloys. Figure 3 gives our calculated results. The agreement with experiment (Table VII) is rather good. We notice that bowing parameters measured from molecular beam epitaxy (MBE) grown films<sup>39,41</sup> have large values suggesting that those samples may not be perfectly random (see below).

The results  $b = 2.71$  eV for Zn(S,Te) can be compared with the value  $b = 2.94$  eV obtained by Bernard and Zunger<sup>61</sup> using a linear superposition of band gaps of

$$E_g(1/2) = \sum_{n=0}^4 P^{(n)}(1/2) E_g[\text{ZnS}_n\text{Te}_{4-n}], \quad (14)$$

where  $P^{(n)}(1/2)$  is the probability of finding the cluster  $\text{ZnS}_n\text{Te}_{4-n}$  at  $x = 1/2$ . For Zn(S,Se) and Zn(Se,Te) Bernard and Zunger<sup>61</sup> used in Eq. (14) only the  $n = 2$  data, finding  $b = 0.39$  eV and  $b = 1.96$  eV, to be compared with the more accurate current values of  $b = 0.50$  eV and  $b = 1.14$  eV, respectively.

Comparing now the bowing in mixed-anion chalcopyrites [Fig. 2(a)] with that in mixed-anion Zn chalcogenides (Fig. 3) we see the same trend  $b(\text{S,Se}) < b(\text{Se,Te}) < b(\text{S,Te})$ , but a significant *reduction* in bowing in the chalcopyrites relative to the II-VI zinc-blende alloys. This trend is analyzed in the next section.

#### E. Analysis of bowing coefficients

Optical bowing in semiconductor alloys is caused by the difference of volume deformation potentials of the constituents and coupling of folded states through the perturbation potential  $\Delta V$ .<sup>47,49,82</sup> Here,  $\Delta V$  is the difference between the alloy potential and the average potential of the constituents.

For direct band-gap semiconductors, the top of the valence band is mostly an anion  $p$ -like state (with some cation  $p$  and  $d$  characters), while the bottom of the conduction band is mostly a cation  $s$  and anion  $s$  state. The  $\Delta V$ -induced *intra-band* coupling within the conduction band and within the valence band lowers the CBM and raises the VBM, thus *reducing* the band gap relative to the average of the constituents. On the other hand,  $\Delta V$ -induced *interband* coupling between the conduction and the valence bands lowers the VBM and raises the CBM, thus *increasing* the band gap. For most semiconductor alloy, the intraband coupling between states of the same orbital character is much stronger than the interband coupling, so alloying reduces the band gap and the bowing  $b$  is positive. Note that  $\Delta V$  has a component arising from the *chemical* differences between the constituents  $A$  and  $B$ , and a component due to the size mismatch between the  $A$  and  $B$  atoms. When two compounds have large difference in their atomic potential or large difference in their size, the optical bowing is expected to be large. The atomic potential disparity between the two constituents is reflected by the differences of their atomic valence eigenvalues. In Table V we show our calculated LDA atomic valence eigenvalues  $\epsilon_s$ ,  $\epsilon_p$ , and  $\epsilon_d$  of elements studied in this paper. The size mismatch of the constituents can be inferred from the mismatch of their lattice constants.

In *mixed-anion alloys* the level repulsion occurs both in the valence bands and in the conduction bands. For the mixed-anion alloys studied here [Fig. 2(a)], CuIn(S,Se) has a rather small bowing, while the bowings for CuIn(Se,Te) and CuIn(S,Te) are large. This is because (i) the  $s$  chemical potential difference between S and Se is small ( $\sim 0.2$  eV), while the Te  $s$  potential is about 2 eV higher than the one for S and Se (Table V), (ii) the  $p$  chemical potential difference is smaller between S and Se ( $\sim 0.45$  eV) than between S and Te ( $\sim 1.0$  eV), and (iii) the size mismatch between S and Se is small, while the size mismatch between S and Te is large (Table IV). Thus, the  $\Delta V$ -induced level repulsion increases from (S,Se), (Se,Te), to (Se,Te), and leads to the trend  $b(\text{S,Se}) < b(\text{Se,Te}) < b(\text{S,Te})$  observed in both chalcopyrite alloys and in the II-VI alloys. Strong level repulsion in (S,Te) alloys also causes wave-function localization. We find that in CuIn(S,Te) the top of the valence band is strongly localized on the Te atom with higher  $p$  orbital energy, while the bottom of the conduction band is strongly localized on the S atom with low  $s$  orbital energy. No strong wave-function localization is observed in CuIn(S,Se), which has almost no bowing. The significant *reduction* in bowing in the chalcopyrites relative to the zinc-blende alloys can be understood by noticing that the stronger  $p-d$  coupling in the chalcopyrites reduces their valence-band offset (hence, chemical disparity) more than the Zn chalcogenides (Sec. III B), thus reduces the bowing.

In *mixed-cation alloys* [Fig. 2(b)] most of the level repulsion occurs in the conduction bands. However, due to their relatively large band offset, the Cu(Al,Ga)Se<sub>2</sub> and Cu(Al,In)Se<sub>2</sub> alloys also exhibit significant perturbation in the valence band. This explains why Cu(Al,Ga)Se<sub>2</sub> and Cu(Al,In)Se<sub>2</sub> have relatively larger bowing coefficients ( $b = 0.39$  and  $0.59$  eV, respectively) than Cu(Ga,In)Se<sub>2</sub> ( $b$

TABLE VII. Calculated (top four lines) bowing parameters of Zn chalcogenides alloys in the ordered CuAu, chalcopyrite (CH), and CuPt phases. For comparison we also give the calculated and measured values for random alloys.

Phase	Zn(S,Se)	Zn(Se,Te)	Zn(S,Te)
$b(\text{CuAu})$	0.46	1.44	3.30
$b(\text{CH})$	0.10	0.25	0.61
$b(\text{CuPt})$	1.09	3.15	5.93
$b(\text{random})$	0.50	1.14	2.71
$b_{\text{expt}}(\text{random})$	$\sim 0.50$	1.23–1.50	3.0–3.2

$=0.21$  eV). We also notice that the bowing coefficient of  $\text{Cu}(\text{Ga,In})\text{Se}_2$  is smaller than  $(\text{Ga,In})\text{V}$  (with  $\text{V}=\text{P, As, and Sb}$ ) alloys ( $b \sim 0.5$  eV).<sup>6</sup> This is because in the chalcopyrite system half of the cation sites are occupied by Cu; so the average chemical disparity between the cation atoms in chalcopyrite alloys is reduced relative to zinc-blende alloys. For the  $\text{Cu}(\text{Al,Ga})\text{Se}_2$  and  $\text{Cu}(\text{Al,In})\text{Se}_2$  alloys the chemical disparity and size disparity between Al and Ga, and between Al and In are both increased in the chalcopyrites relative to in III-V alloys (Sec. II B). This contributes to the larger bowing for these two alloys.

#### F. Optical bowing in ordered alloys

Our foregoing discussion centered on the SQS models for *random* alloys. It is interesting to compare the calculated bowing to those found for hypothetical small unit cell *ordered* alloys. Our results for Zn chalcogenides in the ordered CuAu (an  $AB$  superlattice along  $[001]$  direction), chalcopyrite and CuPt (an  $AB$  superlattice along  $[111]$  direction) structures are summarized in Table VII. We see that band gaps (or bowing) depend sensitively on the assumed atomic arrangements. Due to different folding relations in these ordered phases,<sup>82</sup> the bowing of the ordered phases has the following trend

$$b_{\text{CuPt}} > b_{\text{CuAu}} > b_{\text{CH}}, \quad (15)$$

and

$$b_{\text{CuPt}} > b_{\text{Random}} > b_{\text{CH}}. \quad (16)$$

These trends are also found in calculations on many other zinc-blende semiconductor alloys.<sup>47,82</sup> From Eq. (16) we see that if an alloy orders into the CuPt structure, its band gap will be drastically reduced relative to the disordered alloy.<sup>83</sup> In Zn(S,Se), Zn(Se,Te), and Zn(S,Te) alloys, CuPt ordering at  $x=1/2$  can reduce the band gap by up to 0.15, 0.50, and 0.81 eV, respectively, relative to the random alloy. For alloys ordering into the chalcopyrite structure, the band gap is increased relative to the disordered alloy.<sup>84,85</sup>

The same trends of Eqs. (15) and (16) are found in chalcopyrite alloys. For example, in  $\text{CuIn}(\text{Se}_{0.5}\text{Te}_{0.5})_2$  we found a bowing parameter  $b=1.23$  eV when the Se and Te atoms were arranged in the ordered CuAu structure, while  $b=0.17$  eV when the Se and Te were arranged in the ordered chalcopyrite structure. These results differ significantly from the value  $b=0.44$  eV obtained for the simulated *random* structure.

#### IV. SUMMARY

Using first-principles band-structure theory we have studied systematically the (i) alloy mixing enthalpies  $\Delta H$ , (ii) valence- and conduction-band offsets  $\Delta E_v$  and  $\Delta E_c$ , and (iii) alloy bowing coefficients  $b$  for three mixed-anion ( $\text{CuInX}_2$ ,  $X=\text{S,Se,Te}$ ) and three mixed-cation ( $\text{CuMSe}_2$ ,  $M=\text{Al,Ga,In}$ ) chalcopyrite alloys. The random chalcopyrite alloys are represented by an SQS model. We find that (i) for all the chalcopyrite alloys studied here the mixing enthalpy is positive, indicating that for these alloys the ground state at  $T=0$  corresponds to phase separation into the pure chalcopyrite constituents. However, at higher temperature, the disordered phase can be stabilized through entropy. The mixing enthalpy  $\Delta H$  is rather small for (S,Se), (Al,Ga), (Se,Te), and (Ga,In) alloys, suggesting that these alloys will be miscible in the whole composition range and can thus be formed easily. The mixing enthalpy  $\Delta H$  is large for the (S,Te) alloy, suggesting that a large miscibility gap can exist in this system. (ii) For mixed-cation interfaces, most of the band offsets occur in the conduction band, while for mixed-anion interfaces, both  $\Delta E_v$  and  $\Delta E_c$  are large. (iii) The calculated bowing parameters are all positive for alloys studied here, and are in good agreement with the most reliable experimental data for stoichiometric alloys.  $\text{CuIn}(\text{S,Te})$  and  $\text{CuIn}(\text{Se,Te})$  alloys have large bowing coefficients due to the large chemical disparity and size mismatch in their mixed atoms. (iv) The difference of bowing coefficients and band offsets between the mixed-anion chalcopyrite systems and the corresponding zinc-blende systems are explained in terms of the larger  $p-d$  coupling in chalcopyrite systems. Bowing parameters for ordered Zn chalcogenide alloys (in CuAu, CuPt, and chalcopyrite structure) are predicted. The band alignment between  $\text{CuInSe}_2$  and  $\text{CuInSe}_2$ -derived ordered vacancy compounds are also presented.

#### ACKNOWLEDGMENTS

We thank Professor L. G. Ferreira for verifying the SQS structure for the mixed-cation chalcopyrite alloy. This work was supported in part by U.S. Department of Energy, Grant No. DE-AC02-83-CH10093.

<sup>1</sup> J. L. Shay and J. H. Wernick, *Ternary Chalcopyrite Semiconductors* (Pergamon, Oxford, 1975).

<sup>2</sup> L. Garbato, F. Ledda, and R. Rucci, *Prog. Cryst. Growth Charact.* **15**, 1 (1987).

<sup>3</sup> J. E. Jaffe and A. Zunger, *Phys. Rev. B* **28**, 5822 (1983).

<sup>4</sup> J. E. Jaffe and A. Zunger, *Phys. Rev. B* **29**, 1882 (1984), and references therein.

<sup>5</sup> J. K. Furdyna, *J. Appl. Phys.* **64**, R29 (1988), and references therein.

<sup>6</sup> *Landolt-Bornstein: Numerical Data and Functional Relationships in Science and Technology*, edited by O. Madelung, M. Schulz, and H. Weiss, Vol. 17a,b (Springer, Berlin, 1982).

<sup>7</sup> J. Hedstrom, H. J. Olsen, M. Bodegard, A. Kylner, L. Stolt, D. Hariskos, M. Ruckh, and H. W. Schock, *Proceedings of the 23rd IEEE PV Specialists Conference* (IEEE, New York, 1993), p. 364.

<sup>8</sup> A. M. Gabor, J. R. Tuttle, D. S. Albin, M. A. Contreras, R. Noufi, and A. M. Hermann, *Appl. Phys. Lett.* **65**, 198 (1994).

<sup>9</sup> For a review of device properties, see A. Rothwarf, *Solar Cells* **16**, 567 (1986).

<sup>10</sup> Cited in S. Chichibu *et al.*, *J. Cryst. Growth* **140**, 388 (1994).

<sup>11</sup> L. Roa, C. Rincon, J. Gonzalez, and M. Quintero, *J. Phys. Chem. Solids* **51**, 551 (1990).

- <sup>12</sup>S. Shirakata, A. Ogawa, S. Isomura, and T. Kariya, *Jpn. J. Appl. Phys. Suppl.* **32-3**, 94 (1993).
- <sup>13</sup>L. K. Samanta, D. K. Ghosh, P. S. Ghosh, and S. Chatterjee, *Cryst. Res. Technol.* **28**, 1175 (1993).
- <sup>14</sup>G. H. Chapman, J. Shewchun, J. J. Loferski, B. K. Garside, and R. Beau-lieu, *Appl. Phys. Lett.* **34**, 735 (1979).
- <sup>15</sup>I. V. Bodnar, B. V. Korzun, and A. I. Lukomskii, *Phys. Status Solidi B* **105**, K143 (1981).
- <sup>16</sup>M. Quintero and J. C. Woolley, *J. Appl. Phys.* **55**, 2825 (1984).
- <sup>17</sup>B. Abid, J. R. Gong, H. G. Goslowsky, and K. J. Bachmann, *Proceedings of the 19th IEEE PV Specialists Conference* (IEEE, New York, 1987), p. 1305.
- <sup>18</sup>J. Avon, K. Yoodee, and J. C. Woolley, *Nuovo Cimento D* **2**, 1858 (1983).
- <sup>19</sup>S. Chatraphorn, T. Panmatarite, S. Pramatus, A. Prichavudhi, R. Kritaya-kirana, J.-O. Berananda, V. Sa-yakanit, and J. C. Woolley, *J. Appl. Phys.* **57**, 1791 (1985).
- <sup>20</sup>M. Quintero, R. Tovar, E. Guerrero, F. Sanchez, and J. C. Woolley, *Phys. Status Solidi A* **125**, 161 (1991).
- <sup>21</sup>P. Grima, M. Quintero, C. Rincon, and J. C. Woolley, *Solid State Commun.* **67**, 81 (1988).
- <sup>22</sup>N. Tsuboi, S. Kobayashi, F. Kaneko, and T. Maruyama, *Jpn. J. Appl. Phys.* **27**, 972 (1988).
- <sup>23</sup>S. Shirakata, S. Chichibu, R. Sudo, A. Ogawa, S. Matsumoto, and S. Isomura, *Jpn. J. Appl. Phys.* **32**, L1304 (1993).
- <sup>24</sup>I. V. Bodnar and A. I. Lukomskii, *Phys. Status Solidi A* **98**, K165 (1986).
- <sup>25</sup>I. V. Bodnar, A. P. Bologa, and B. V. Korzun, *Phys. Status Solidi B* **109**, k31 (1982).
- <sup>26</sup>T. F. Ciszek, R. Bacewicz, J. Durrant, S. K. Deb, and D. Dunlavy, *Proceedings of the 19th IEEE PV Specialists Conference* (IEEE, New York, 1987), p. 1448; R. Bacewicz, J. Durrant, T. F. Ciszek, and S. K. Deb, in *Ternary and Multinary Compounds*, edited by S. K. Deb and A. Zunger (MRS, Pittsburgh, 1987), p. 155.
- <sup>27</sup>J. Durran, SERI Technical Report RR-212-3064, 1987.
- <sup>28</sup>B. Dimmler, H. Dittich, R. Menner, and H. W. Schock, *Proceedings of the 19th IEEE PV Specialists Conference* (IEEE, New York, 1987), p. 1454.
- <sup>29</sup>W. S. Chen, J. M. Stewart, B. J. Stanbery, W. E. Devaney, and R. A. Mickelsen, *Proceedings of the 19th IEEE PV Specialists Conference* (IEEE, New York, 1987), p. 1445.
- <sup>30</sup>D. S. Albin, J. J. Carapella, J. R. Tuttle, and R. Noufi, *Mater. Res. Soc. Symp. Proc.* **228**, 267 (1991).
- <sup>31</sup>T. Tinoco, C. Rincon, M. Quintero, and G. S. Perez, *Phys. Status Solidi A* **124**, 427 (1991).
- <sup>32</sup>T. Yamaguchi, J. Matsufusa, and A. Yoshida, *Jpn. J. Appl. Phys.* **31**, L703 (1992).
- <sup>33</sup>C. Larez, C. Bellabarba, and C. Rincon, *Appl. Phys. Lett.* **65**, 1650 (1994).
- <sup>34</sup>L. G. Suslina, D. L. Fedorov, S. G. Konnikov, F. F. Kodzhespirow, A. A. Andreev, and E. G. Shariia, *Fiz. Tekh. Poluprovodn.* **11**, 1934 (1977) [*Sov. Phys. Semicond.* **11**, 1132 (1977)].
- <sup>35</sup>A. Ebina, E. Fukunaga, and T. Takahashi, *Phys. Rev. B* **10**, 2495 (1974); L. Soonckindt, D. Etienne, J. P. Marchand, and L. Lassabatere, *Surf. Sci.* **86**, 378 (1979); D. Etienne, M. de Murcia, and G. Bougnot, *Thin Solid Film* **70**, 285 (1980).
- <sup>36</sup>R. Mach, P. Flögel, L. G. Suslina, A. G. Areshkin, J. Maeger, and G. Voigt, *Phys. Status Solidi B* **109**, 607 (1982); J. E. Nicholls, J. J. Davies, N. R. J. Podton, R. Mach, and G. O. Müller, *J. Phys. Chem.* **18**, 455 (1985).
- <sup>37</sup>A. A. El Shazly, M. M. H. El Naby, M. A. Kenawy, M. M. El Nahass, H. T. El Shair, and A. M. Ebrahim, *Appl. Phys. A* **36**, 51 (1985).
- <sup>38</sup>A. Ebina, M. Yamamoto, and T. Takahashi, *Phys. Rev. B* **6**, 3786 (1972).
- <sup>39</sup>M. J. S. P. Brasil, R. E. Nahory, F. S. Turco-Sandroff, H. L. Gilchrist, and R. J. Martin, *Appl. Phys. Lett.* **58**, 2509 (1991).
- <sup>40</sup>R. Hill and D. Richardson, *J. Phys. C* **6**, L115 (1973).
- <sup>41</sup>K. S. Wong, H. Wang, I. K. Sou, Y. W. Chan, and G. K. L. Wong, *Proceedings of 22nd International Conference on the Physics of Semiconductor* (World Scientific, Singapore, 1994), p. 349.
- <sup>42</sup>P. Hohenberg and W. Kohn, *Phys. Rev.* **136**, B864 (1964); W. Kohn and L. J. Sham, *ibid.* **140**, A1133 (1965).
- <sup>43</sup>K. Hass, L. C. Davis, and A. Zunger, *Phys. Rev. B* **42**, 3757 (1990).
- <sup>44</sup>Z. Q. Li and W. Potz, *Phys. Rev. B* **46**, 2109 (1992).
- <sup>45</sup>K. A. Mader and A. Zunger, *Appl. Phys. Lett.* **64**, 2882 (1994); *Phys. Rev. B* (to be published).
- <sup>46</sup>J. M. Sanchez, F. Ducastelle, and D. Gratias, *Physica* **182A**, 334 (1984).
- <sup>47</sup>A. Zunger, S.-H. Wei, L. G. Ferreira, and J. E. Bernard, *Phys. Rev. Lett.* **65**, 353 (1990); S.-H. Wei, L. G. Ferreira, J. E. Bernard, and A. Zunger, *Phys. Rev. B* **42**, 9622 (1990).
- <sup>48</sup>R. Magri, S. Froyen, and A. Zunger, *Phys. Rev. B* **44**, 7947 (1991).
- <sup>49</sup>S.-H. Wei and A. Zunger, *Phys. Rev. B* **43**, 1662 (1991); 14272 (1991).
- <sup>50</sup>Z. W. Lu, S.-H. Wei, and A. Zunger, *Phys. Rev. B* **44**, 10470 (1991).
- <sup>51</sup>Z. W. Lu, S.-H. Wei, and A. Zunger, *Phys. Rev. B* **45**, 10314 (1992).
- <sup>52</sup>P. N. Keating, *Phys. Rev.* **145**, 637 (1966).
- <sup>53</sup>J. L. Martins and A. Zunger, *Phys. Rev. B* **30**, 6217 (1987).
- <sup>54</sup>L. Vegard, *Z. Phys.* **5**, 17 (1921).
- <sup>55</sup>H. W. Spiess, V. Haeberlin, G. Brandt, A. Rauber, and J. Schneider, *Phys. Status Solidi B* **62**, 183 (1974).
- <sup>56</sup>S.-H. Wei and H. Krakauer, *Phys. Rev. Lett.* **55**, 1200 (1985), and references therein.
- <sup>57</sup>D. M. Ceperly and B. J. Alder, *Phys. Rev. Lett.* **45**, 566 (1980).
- <sup>58</sup>J. P. Perdew and A. Zunger, *Phys. Rev. B* **23**, 5048 (1981).
- <sup>59</sup>S. Froyen, *Phys. Rev. B* **39**, 3168 (1989).
- <sup>60</sup>J. J. Hopfield, *J. Phys. Chem. Solids* **15**, 97 (1960).
- <sup>61</sup>J. E. Bernard and A. Zunger, *Phys. Rev. B* **36**, 3199 (1987).
- <sup>62</sup>S.-H. Wei and A. Zunger, *Phys. Rev. Lett.* **59**, 144 (1987).
- <sup>63</sup>S.-H. Wei and A. Zunger, *Phys. Rev. B* **37**, 8958 (1988).
- <sup>64</sup>S.-H. Wei, in *II-VI Semiconductor Compounds*, edited by M. Jain (World Scientific, Singapore, 1993).
- <sup>65</sup>A. J. Nelson, C. R. Schwerdfeger, S.-H. Wei, A. Zunger, D. Rioux, R. Patel, and H. Hochst, *Appl. Phys. Lett.* **62**, 2557 (1993).
- <sup>66</sup>A. Franceschetti, S.-H. Wei, and A. Zunger, *Phys. Rev. B* **50**, 17797 (1994).
- <sup>67</sup>F. H. Pollak and M. Cardona, *Phys. Rev.* **172**, 816 (1968).
- <sup>68</sup>C. G. Van de Walle, *Phys. Rev. B* **39**, 1871 (1989).
- <sup>69</sup>S.-H. Wei and A. Zunger, *Appl. Phys. Lett.* **63**, 2549 (1993).
- <sup>70</sup>J. O. McCaldin, T. C. McGill, and C. A. Mead, *Phys. Rev. Lett.* **36**, 56 (1976).
- <sup>71</sup>S.-H. Wei and A. Zunger (unpublished).
- <sup>72</sup>A. D. Katnani and G. Margaritondo, *J. Appl. Phys.* **54**, 2522 (1983).
- <sup>73</sup>T. Nakayama, *J. Phys. Soc. Jpn.* **61**, 2434 (1992).
- <sup>74</sup>Y. Rajakarunanyake, M. C. Phillips, J. O. McCaldin, D. H. Chow, D. A. Collins, and T. C. McGill, *Proc. SPIE* **1285**, 142 (1990).
- <sup>75</sup>M. Ukita, F. Hiei, K. Nakano, and A. Ishibashi, *Appl. Phys. Lett.* **66**, 209 (1995).
- <sup>76</sup>B. Freytag, *Semicond. Sci. Technol.* **10**, 270 (1995), and references therein.
- <sup>77</sup>D. Schmid, M. Ruckh, F. Grunwald, and H. W. Schock, *J. Appl. Phys.* **73**, 2902 (1993).
- <sup>78</sup>S.-H. Wei and A. Zunger (unpublished).
- <sup>79</sup>A. Zunger and A. J. Freeman, *Phys. Rev. B* **16**, 2901 (1977).
- <sup>80</sup>T. Tinoco, M. Quintero, and C. Rincon, *Phys. Rev. B* **44**, 1613 (1991).
- <sup>81</sup>J. C. Phillips, *Bonds and Bands in Semiconductors* (Academic, New York, 1973).
- <sup>82</sup>S.-H. Wei and A. Zunger, *Phys. Rev. B* **39**, 3279 (1989).
- <sup>83</sup>S.-H. Wei, D. B. Laks, and A. Zunger, *Appl. Phys. Lett.* **62**, 1937 (1993).
- <sup>84</sup>M. A. Ryan, M. W. Peterson, D. L. Williamson, J. S. Frey, G. E. Maciel, and B. A. Parkinson, *J. Mater. Res.* **2**, 528 (1987).
- <sup>85</sup>S.-H. Wei, L. G. Ferreira, and A. Zunger, *Phys. Rev. B* **45**, 2533 (1992).